Hindawi Publishing Corporation
Journal of Nanomaterials
Volume 2015, Article ID 563587, 7 pages
http://dx.doi.org/10.1155/2015/563587

Research Article

WO_3 Nanoplates Film: Formation and Photocatalytic Oxidation Studies

Chin Wei Lai

Nanotechnology & Catalysis Research Centre (NANOCAT), 3rd Floor, Block A, Institute of Postgraduate Studies (IPS), University of Malaya, 50603 Kuala Lumpur, Malaysia

Correspondence should be addressed to Chin Wei Lai; cwlai@um.edu.my

Received 13 April 2015; Accepted 24 May 2015

Academic Editor: Kezhen Qi

High surface area of tungsten oxide (WO_3) nanoplates films was prepared via simple electrochemical anodization technique by controlling the fluoride content (NH_4F) in electrolyte. The design and development of WO_3-based nanostructure assemblies have gained significant interest in order to maximize specific surface area for harvesting more photons to trigger photocatalytic oxidation reaction. This study aims to determine the optimum content of NH_4F in forming WO_3 nanoplates on W film with efficient photocatalytic oxidation reaction for organic dye degradation by utilizing our solar energy. The NH_4F was found to influence the chemical dissolution and field-assisted dissolution rates, thus modifying the final morphological of WO_3-based nanostructure assemblies film. It was found that 0.7 wt% of NH_4F is the minimum amount to grow WO_3 nanoplates film on W film. The photocatalysis oxidation experimental results showed that WO_3 nanoplates film exhibited a maximum degradation of methyl orange dye (≈75%) under solar illumination for 5 hours. This behavior was attributed to the better charge carriers transportation and minimizes the recombination losses with specific surface area of nanoplates structure.

1. Introduction

Nowadays, serious environmental pollution is the most threatening problem to humankind, especially residual dyes pollution from textile industries. Therefore, executing research for the removal of pollutants from wastewater has been the passion for scientists all over the world, which can provide us a cost-effective method for water decontamination applications. In this manner, photocatalytic oxidation system has attracted great interest from science community as the most promising way to solve the environmental problems by utilizing our sunlight, especially getting rid of residual dyes pollutants from wastewater stream [1–3]. To date, a number of semiconductor materials have been investigated to meet the requirement of the photocatalytic oxidation system [2–5]. Unfortunately, poor visible light absorption and rapid recombination of charge carriers limit the widespread use of semiconductor materials [4–7]. However, some success has been achieved by employing small band gap of oxide semiconductor material, especially tungsten oxide (WO_3) [8–10]. WO_3 has attracted considerable scientific interest due to its unique chemical and physical properties [8, 10–12]. WO_3 possesses many advantages and unique functional properties compared with other semiconducting materials, such as small band gap energy (2.4–2.8 eV), deeper valence band (+3.1 eV), stable physicochemical properties, and strong photocorrosion stability in aqueous solution as well as stable recyclability performance [11–14].

However, WO_3 is still far from becoming a practical semiconductor for photocatalysis system due to its rapid recombination of photoinduced electron-hole pairs [15, 16]. Since the process of electrons transfer to the conduction band of the oxide is a surface phenomenon, it is anticipated that the larger the specific surface area of the semiconductor is, the more the photoinduced electron-hole pairs can be transferred to the oxide's surface for activating the photocatalysis reactions. Thus, modification of WO_3 film to improve the recombination losses of charge carriers is necessary and crucial. Numerous studies have reported that designing and modifying WO_3 structure into nanodimension or nanostructure could overcome the recombination losses of charge carriers and improve the photocatalysis oxidation

performance significantly [15–17]. Theoretically, manipulation of an oxide semiconductor material at atomic, molecular, and macromolecular scales will change its physical, chemical, and functional properties significantly, which is different to those at larger scale [18]. As a result, it could be expected that band gap narrowing effects could expand the range of excitation light to the visible region and provide sites that slow down the recombination of charge carriers that can be expected. Therefore, it is inferred that high specific surface area of WO_3 nanostructure film could enhance the photocatalytic oxidation activity [17, 19]. Continuous efforts have been exerted to improve equilibrium reactions by simultaneous control of oxidation and dissolution reactions to grow WO_3 nanostructure film by controlling the fluoride content during electrochemical anodization. To the best of our knowledge, detailed studies on WO_3 nanostructure film via electrochemical anodization technique and their photocatalytic oxidation reaction are still lacking. This study aims to determine the optimum content of fluoride to obtain the desired WO_3 nanoplates film for the best photocatalytic oxidation performance.

2. Experimental Procedure

In the present study, 99.5% purity of tungsten (W) film with 0.01 mm thickness was cut into desired dimension (1 cm × 5 cm). Then, the W film was immersed in the ethanol and then sonicated in the ultrasonic bath for 10 min. The following step was rinsing with DI water and drying at room temperature. In this manner, the cleanliness and purity of initial W film are very important to ensure that all W films were free from contaminants, such as finger print or debris which might affect the uniform growth of nanostructures. As a matter of fact, electrolyte composition has significant influence on the morphology-controlled growth for WO_3 nanostructures. The electrochemical anodization process (anodic oxidation) was performed in a two electrodes cell with W film as the anode and the platinum rod as the counter electrode in an organic ethylene glycol containing different amount of ammonium fluoride (NH_4F, Merck) from 0.1 wt% to 0.7 wt%. The mixture electrolyte was stirred for 1 h in order to make sure that all NH_4F fully dissolved in ethylene glycol prior to anodization process. The electrochemical anodization was fixed at 60 V with sweep rate 0.1 V/s for 60 min.

The clean W foil and the platinum electrode were immersed in the electrolyte and anodized at 40 V after voltage sweep from 0 to 40 V with sweep rate 0.1 V/s. For every set of experiments, the distance between platinum and W foil was fixed to 3 cm. The electrolyte was stirred continuously using magnetic stirrer during the anodization stage. After anodization process, the anodized sample was washed with acetone. The purpose of cleaning with acetone is to remove the remaining electrolytes and precipitates that cover the oxide layer on W film. Annealing is a heat treatment process where the amorphous structure of the WO_3 can be transformed to crystalline phase. In this work, annealing at 400°C for 4 hours was applied in order to induce monoclinic phase to the anodic WO_3 film.

The morphologies of anodic WO_3 film were then characterized by using field emission scanning electron microscopy (FESEM Zeiss SUPRA 35VP). The elemental analysis of the desired WO_3 nanoplates film was determined using energy dispersion X-ray (EDX) equipped in the FESEM. The phase determination of the anodic layer was determined by an X-ray diffraction (XRD) using Philips, PW1729, operated at 45 kV and 40 mV. A Raman spectrum was obtained at room temperature using an LS 55 luminescence spectrometer (Jobin-Yvon HR 800UV).

The photocatalytic oxidation studies were performed by dipping sintered anodic sample in 100 mL of 30 ppm methyl orange (azo dye) solution in a custom-made photoreactor system consisting of quartz glass. The samples were located in the reactor for 30 minutes in dark environment in order to reach the equilibrium adsorption; the samples were then photoirradiated at room temperature by using a 300 W xenon arc tunable light source to produce a largely continuous and uniform spectrum across the entire UV-visible-infrared wavelength range. The distance from the light source to the reactor was fixed at 50 mm. In order to evaluate the photocatalysis oxidation analysis of methyl orange after solar irradiation, 5 mL solution was withdrawn from quartz tubes for every 30 minutes. A UV spectrometer was used to measure the concentration of the degraded methyl orange solution.

3. Results and Discussion

In the present study, dissolution reaction plays a crucial role in the formation of nanostructure and ultimately defines their structural characteristics [20]. In fact, fluoride (F^-) ions in the form of hydrofluoric acid (HF), potassium fluoride (KF), sodium fluoride (NaF), and ammonium fluoride (NH_4F) have been extensively used to control the dissolution reaction in the anodic growth of WO_3 nanoplates film. In this manner, F^- ions were used to promote conditions that will dissolve the anodic oxides while the anodic bias permanently provides new oxide layer growth. After that, a steady state between oxide formation and dissolution will occur, and then equilibrium can be achieved leading to nanostructure oxide layer [16, 17]. However, the nanostructure formed in electrolyte containing Na^+ resulted in the formation of a precipitated layer that is composed of Na salt while the use of HF, KF, and NaF is limited due to poor solubility of these salts in alcohol-based electrolyte [21]. These emphasize the essentiality of choosing NH_4F as F^- source for anodic oxidation of W foil in ethylene glycol electrolyte. Thus, ethylene glycol containing different amounts of NH_4F from 0.1 wt% up to 0.7 wt% was investigated. The variations in surface morphologies of the anodic WO_3 film formed in ethylene glycol containing different NH_4F concentrations are shown in Figures 1(a)–1(d). The anodic oxidation in 0.1 wt% F^- ion electrolyte resulted in the formation of a thin and compact oxide as presented in Figure 1(a). Meanwhile, this indicates that a low F^- ions concentration (0.1 wt% NH_4F) is insufficient in forming a pit on the oxide layer because of inactive chemical dissolution reaction. Figure 1(b) shows the FESEM image of the anodized W film prepared in ethylene glycol containing 0.3 wt% of

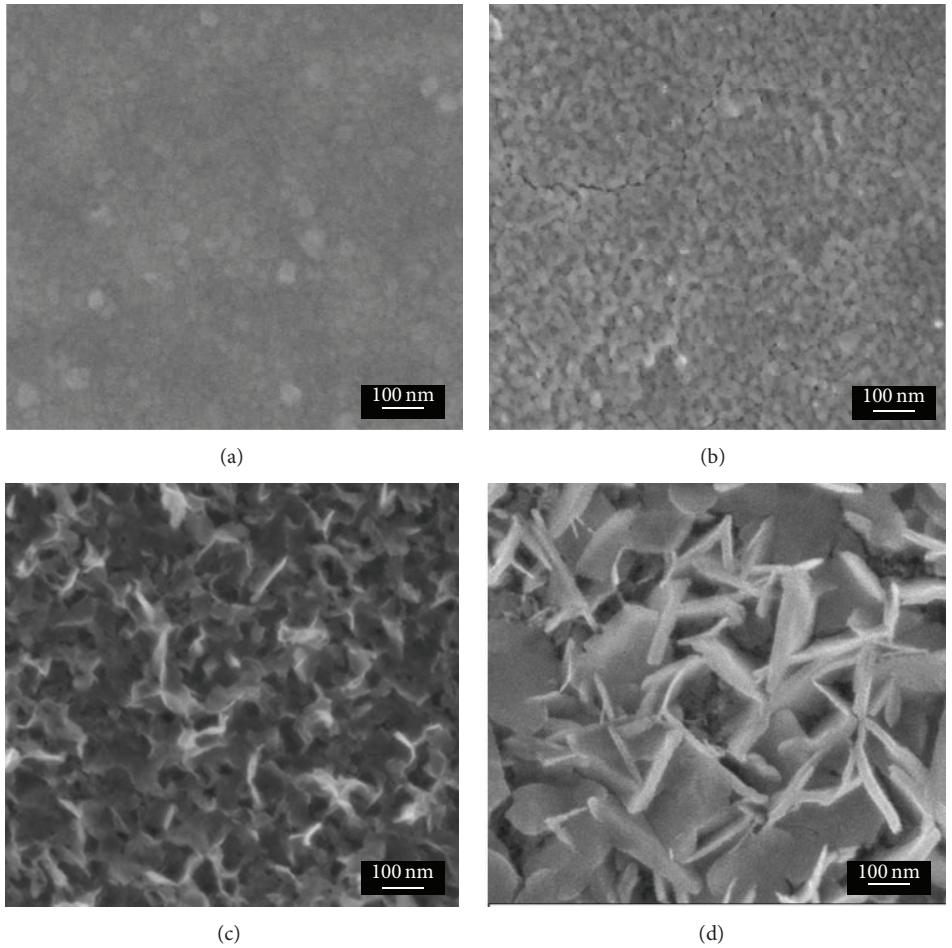

Figure 1: FESEM images of the W film anodized in ethylene glycol electrolyte for 1 h at 60 V using different content of NH_4F: (a) 0.1 wt%; (b) 0.3 wt%; (c) 0.5 wt%; and (d) 0.7 wt%.

NH_4F. The surface containing irregular features of oxide layer instead of ordered nanopores was observed. The inadequate F^- levels probably caused incomplete chemical dissolution and oxidation at the interface between W and the barrier layer. For the 0.5 wt% NH_4F, thick and irregular features of nanoporous oxide layer were observed, which indicates that the amount of F^- ions present in the ethylene glycol was sufficient to trigger the field-assisted dissolution reaction occurring on the W film's surface as shown in Figure 1(c). In this case, the resultant F^- ions start to etch the oxide layer on W film and started to grow nanostructure oxide layer. When the NH_4F content was increased to 0.7 wt%, it was found that a WO_3 layer with nanoplate-like morphology with meso/microgaps between the layers was successfully formed. The nanoplate-like morphology was typically in square shape and exhibited an average edge width of 20 nm with a thickness of approximately 250 nm, as shown in Figure 1(d).

It could be understood that the migration of F^- ions across the oxide/electrolyte interface dominated the chemical dissolution and leads to further acidification to develop a nanoplate-like morphology on W film. The increase in F^- content could significantly accelerate the growth of nanostructure oxide layer. The equilibrium growth of well-defined nanoplate-like morphology on W film was achieved by incorporating 0.7 wt% of NH_4F into the ethylene glycol. A thin barrier layer formed at such condition allowed the rapid growth of nanoplate-like morphology by fast movement of the oxide/metal interface to the metal surface inwards. This resulted in the formation of nanoplate-like morphology with meso/microgaps between the layers on W film.

EDX analysis was conducted to determine the average atomic percent (at%) of the carbon elements present in the anodic WO_3 film with different content of NH_4F. The results from EDX spectra are presented in Table 1. All of the anodic WO_3 film exhibited the peaks of W, O, and C from EDX spectrum (not shown). The intensity of the C peak increased upon higher content of F^- species corresponding to higher C content on the WO_3 film. The EDX results of anodic WO_3 film synthesized in the NH_4F content of 0.1 wt%, 0.3 wt%, 0.5 wt%, and 0.7 wt% show the carbon content of 1.30 at%, 1.67 at%, 2.17 at%, and 2.45 at%, respectively. This result was understandable because the carbon loading rate into the anodic WO_3 film was increasing via the pyrogenation process of organic ethylene glycol during anodization stage [22]. In this manner, organic ethylene glycol was oxidized to carbonate-type species, which get absorbed on the wall

Table 1: Average at% of WO_3 nanostructure film using different content of NH_4F obtained by EDX analysis.

Content of NH_4F (wt%)	W (wt%)	O (wt%)	C (wt%)
0.1	89.39	9.31	1.30
0.3	88.93	9.40	1.67
0.5	88.75	9.08	2.17
0.7	88.21	9.34	2.45

surface of WO_3 layer. Then, these carbonate-type species were reduced to carbon species during heat treatment process and diffused into the lattice of WO_3 [23]. Thus, the presence of the carbon species was found within anodic WO_3 film.

In order to obtain the comprehension on the influence of oxidizing and etching agents to the growth behavior of the anodic WO_3 nanostructure on W film, anodic oxidation of the W foil was carried out in organic ethylene glycol containing different NH_4F concentrations. The difference in morphology of the anodic WO_3 nanostructure can be explained by referring to the current density profile (*J-t*) throughout the anodization process and was plotted in Figure 2. It was found that the *J-t* curves for both samples synthesized at low concentration of NH_4F of 0.1 wt% and 0.3 wt% showed similar trends and the current density was shown at the 0.0011 A/cm^2 and 0.0017 A/cm^2, respectively. The similar trends presented in *J-t* curves, corresponding to the formation behavior of irregular features oxide layer on W film without porous structure. On the other hand, anodic samples synthesized at high concentration of NH_4F of 0.5 wt% and 0.7 wt% of NH_4F showed the highest current density of 0.0035 A/cm^2 and 0.0044 A/cm^2, respectively, in *J-t* curves. This is ascribed to the high diffusivity and the ion concentration in the electrolyte because of the continuous increase in fluoride species, which led to enhancing conductivity of the solution [24, 25]. The gradual increase in *J* resulted from migration of F^- to thick initial oxide layer inwards, indicating a rapid ionic mobility in electrolyte and a large number of charge carriers transported across a barrier layer. As a result, high chemical dissolution and etching processes on the oxide/metal interface occurred and allowed formation of nanoplate-like morphology on W film. This condition indicates the great effect of ionic mobility and the number of charge carriers on the growth behavior and structural characteristics of nanoplate-like morphology.

Crystal structures of anodic WO_3 nanostructure film play a crucial role in determining their photocatalytic oxidation properties [19]. Thus, as-grown nanotube arrays were subsequently heat-treated at 400°C for 4 hours in argon gas atmosphere to form crystalline structure. In this work, the nanoplates films were formed to be stable up to 400°C. The crystallization of the W substrate disturbed the nanostructure architecture causing the nanoplates to collapse at high annealing temperature. The reason for the collapse was mainly attributed to the phase protrusion emerging from the metal structure at high temperature (500°C or higher). In the present study, XRD analysis was used to investigate the crystallization and phase transition of anodic WO_3 nanostructure film (Figure 3). The Bragg reflection of

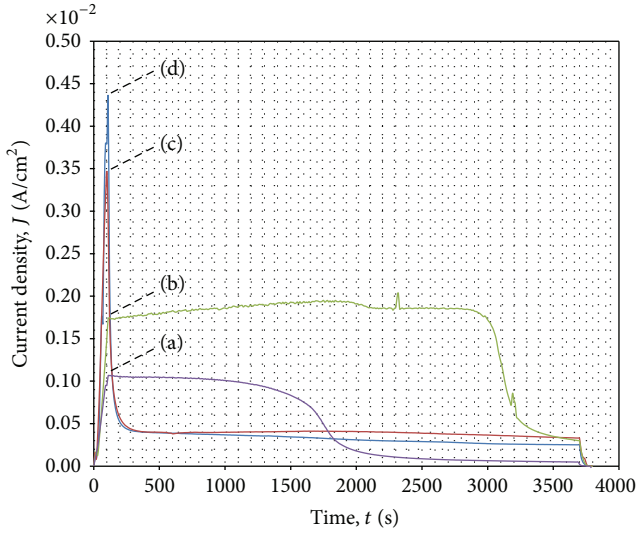

Figure 2: Current density-time behavior during anodization of W film in ethylene glycol containing different content of NH_4F at 60 V for 1 h: (a) 0.1 wt%, (b) 0.3 wt%, (c) 0.5 wt%, and (d) 0.7 wt%.

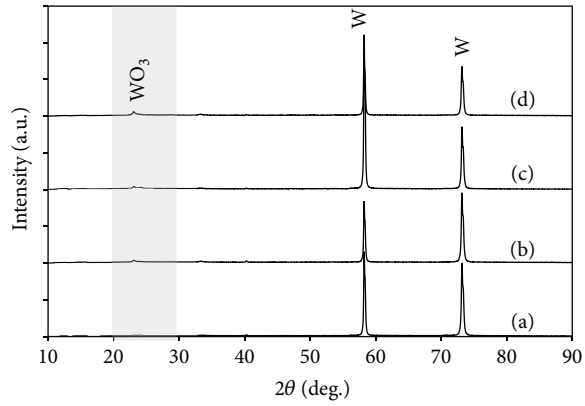

Figure 3: The full-range XRD pattern for the anodic WO_3 nanostructure film anodized in an ethylene glycol containing different NH_4F: (a) 0.1 wt%, (b) 0.3 wt%, (c) 0.5 wt%, and (d) 0.7 wt% at 60 V for 1 h after applying heat treatment of 400°C for 4 h.

W phase was detected at 2θ values of 58.27° and 72.21° in the entire XRD patterns, corresponding to (200) and (211) crystal planes, respectively. The presence of W phase was identified by ICDD file of 04-0806. The intensity of the W peaks at 72.21° decreased with increasing concentration of NH_4F, indicating the reduced crystallinity of the W phase with increasing the WO_3 layer on W film. In addition, small additional peaks could be observed from the XRD patterns at 23.52°, corresponding to (001) crystal plane of orthorhombic tungstate ($WO_3 \cdot H_2O$). It is worth noting that the structure of a nanoplate starts with the orthorhombic $WO_3 \cdot H_2O$ phase after heat treatment of 400°C, which has a layered structure with sheets of distorted W-O octahedral units sharing corners [26, 27]. These anodic WO_3 nanoplate-like morphologies were bonded with each other by the hydrogen atoms of water molecules bonded with the oxygen

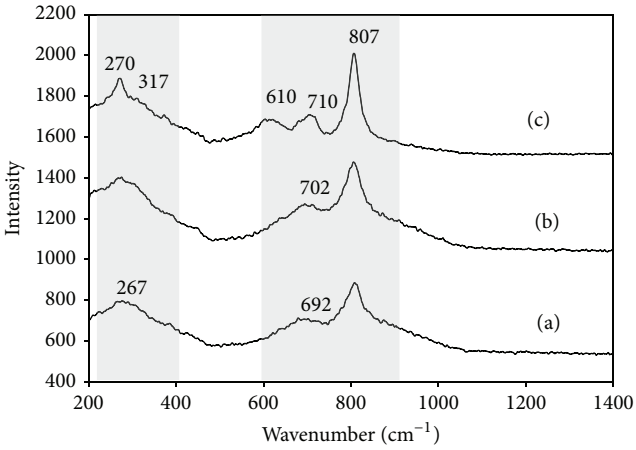

Figure 4: Raman spectra of anodic WO_3 nanostructure films anodized in an ethylene glycol containing different NH_4F: (a) 0.1 wt%, (b) 0.5 wt%, and (c) 0.7 wt% at 60 V for 1 h after applying heat treatment of 400°C for 4 h.

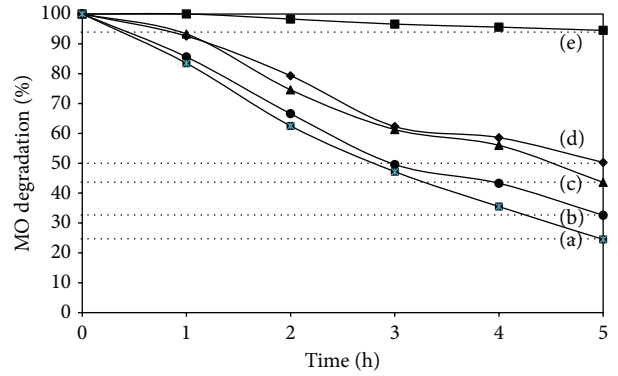

Figure 5: Photocatalytic degradation of MO aqueous dye solution under solar irradiation over anodic WO_3 samples synthesized in an ethylene glycol containing different NH_4F at 60 V for 1 h: (a) 0.7 wt%, (b) 0.5 wt%, (c) 0.3 wt%, (d) 0.1 wt%, and (e) control sample (blank sample).

atoms in the adjacent W-O layer [28]. The crystallographic structure of the WO_3 nanoplate-like morphology changed from the amorphous phase into orthorhombic $WO_3 \cdot H_2O$ in ambient argon atmosphere up to 400°C.

In this study, Raman analysis has been used to determine and understand the structural changes of anodic WO_3 nanostructure film upon different content of NH_4F. There are three frequency regions that can be individuated from the Raman spectra and could be detected for tungsten trioxide (WO_3) crystalline phase [29]. The increment in the PL intensity for the anodic WO_3 nanostructure film synthesized at high NH_4F content was observed from the Raman spectra as presented in Figure 4. The peaks appearing at 270 cm^{-1} and 317 cm^{-1} infer the stretching modes of the W-O-W bending vibrations of the bridging oxygen. The other peaks observed at 710 cm^{-1} and 807 cm^{-1} could be attributed to the symmetric and asymmetric vibrations of W^{6+}-O bonds (O-W-O stretching modes). Phase transition is between monoclinic and orthorhombic WO_3 within the intense peak (710 cm^{-1} and 807 cm^{-1}) in the WO_6 octahedral unit [30].

The photodegradation of methyl orange (MO) aqueous dye solution in the presence of anodic WO_3 film with various surface areas and morphologies is summarized in Figure 5. These results show the decay in MO aqueous dye solution with 300 W xenon arc tunable light sources in the presence of synthesized anodic film under different NH_4F content. The strongest photocatalytic activity of MO aqueous dye solution with 75% degradation within 5 hours of exposure time could be observed for the nanoplate-like morphology with meso/microgaps between the layers on W film, which is relatively high, compared to the other samples. These results are in line with the literatures, which suggested that the high photodegradation of MO aqueous dye solution is mainly attributed to the strong light scattering effects and high specific surface area for incident light absorption from any direction [15–17]. The larger active surface area proximal to the MO aqueous dye solution enhances the generation of photoinduced electron and hole pairs, which are able to generate highly active radicals (hydroxyl radicals $^{\bullet}OH$ and superoxide anions $O_2^{\bullet -}$) that are able to undergo secondary reactions for degradation purpose. The $O_2^{\bullet -}$ or $HO^{\bullet}$ radicals will then react with MO aqueous dye solution and subsequently decompose into harmless substances (product) in the presence of carbon dioxide (CO_2) and water (H_2O). In addition to that, the presence of the C species found within anodic WO_3 film also played an important role in improving its photocatalytic activity. The mixing of the C p states with the O 2p states shifted the valence band edge upward and narrow down the band gap energy of the anodic WO_3 film. Theoretically, carbon doping within anodic WO_3 film formed fewer recombination centers nearby the catalyst's surface; thus, the photodegradation of MO aqueous dye solution could be enhanced significantly.

4. Conclusion

In the present study, anodic WO_3 nanoplate-like morphology with meso/microgaps between the layers was successfully formed in an ethylene glycol containing 0.7 wt% of NH_4F at 60 V for 1 h. The migration of F^- ions across the oxide/electrolyte interface dominated the chemical dissolution and leads to further acidification to develop a nanoplate-like morphology on W film. The resultant anodic sample exhibited the promising photocatalysis oxidation reactions towards the azo dye degradation (methyl orange) with about 75% degradation rate within 5 hours. The anodic WO_3 nanoplate-like morphology with meso/microgaps between the layers showed strong light scattering effects and high specific surface area for incident light absorption from any direction, which eventually enhances the photocatalysis reactions.

Conflict of Interests

The author declares that there is no conflict of interests regarding the publication of this paper.

Acknowledgments

The author would like to thank University of Malaya for funding this research work under University of Malaya Research Grant (UMRG) (RP022-2012D), Postgraduate Research Grant Scheme (PPP) (PG052-2014B), and Fundamental Research Grant Scheme (FRGS) (FP055-2013B).

References

[1] A. Fujishima, X. Zhang, and D. A. Tryk, "TiO_2 photocatalysis and related surface phenomena," *Surface Science Reports*, vol. 63, no. 12, pp. 515–582, 2008.

[2] A. Kubacka, M. Fernández-García, and G. Colón, "Advanced nanoarchitectures for solar photocatalytic applications," *Chemical Reviews*, vol. 112, no. 3, pp. 1555–1614, 2012.

[3] C. W. Lai, J. C. Juan, W. B. Ko, and S. Bee Abd Hamid, "An overview: recent development of titanium oxide nanotubes as photocatalyst for dye degradation," *International Journal of Photoenergy*, vol. 2014, Article ID 524135, 14 pages, 2014.

[4] M. Kitano, M. Matsuoka, M. Ueshima, and M. Anpo, "Recent developments in titanium oxide-based photocatalysts," *Applied Catalysis A: General*, vol. 325, no. 1, pp. 1–14, 2007.

[5] A. Ghicov and P. Schmuki, "Self-ordering electrochemistry: a review on growth and functionality of TiO_2 nanotubes and other self-aligned MOx structures," *Chemical Communications*, no. 20, pp. 2791–2808, 2009.

[6] Y.-C. Nah, I. Paramasivam, and P. Schmuki, "Doped TiO_2 and TiO_2 nanotubes: synthesis and applications," *ChemPhysChem*, vol. 11, no. 13, pp. 2698–2713, 2010.

[7] M. Ni, M. K. H. Leung, D. Y. C. Leung, and K. Sumathy, "A review and recent developments in photocatalytic water-splitting using TiO_2 for hydrogen production," *Renewable & Sustainable Energy Reviews*, vol. 11, no. 3, pp. 401–425, 2007.

[8] G. A. Niklasson and C. G. Granqvist, "Electrochromics for smart windows: thin films of tungsten oxide and nickel oxide, and devices based on these," *Journal of Materials Chemistry*, vol. 17, no. 2, pp. 127–156, 2007.

[9] E. L. Runnerstrom, A. Llordés, S. D. Lounis, and D. J. Milliron, "Nanostructured electrochromic smart windows: traditional materials and NIR-selective plasmonic nanocrystals," *Chemical Communications*, vol. 50, no. 73, pp. 10555–10572, 2014.

[10] Y. T. Hsieh, L. W. Chang, C. C. Chang, B. J. Wei, and H. C. Shih, "Novel synthetic route for tungsten oxide nanobundles with controllable morphologies," in *Recent Trend in Electrochemical Science and Technology*, U. K. Sur, Ed., chapter 11, InTech, Rijeka, Croatia, 2012.

[11] X. Zhang, K. Huo, L. Hu, and P. K. Chu, "Fabrication and photocatalytic activity of nanoporous WO_3 film," *Nanoscience and Nanotechnology Letters*, vol. 2, no. 1, pp. 51–57, 2010.

[12] W. Li, J. Li, X. Wang, S. Luo, J. Xiao, and Q. Chen, "Visible light photoelectrochemical responsiveness of self-organized nanoporous WO_3 films," *Electrochimica Acta*, vol. 56, no. 1, pp. 620–625, 2010.

[13] C. W. Lai, S. B. Abd Hamid, and S. Sreekantan, "A novel solar driven photocatalyst: well-aligned anodic WO_3 Nanotubes," *International Journal of Photoenergy*, vol. 2013, Article ID 745301, 6 pages, 2013.

[14] K. Jothivenkatachalam, S. Prabhu, A. Nithya, and K. Jeganathan, "Facile synthesis of WO_3 with reduced particle size on zeolite and enhanced photocatalytic activity," *RSC Advances*, vol. 4, no. 41, pp. 21221–21229, 2014.

[15] L. Meda, G. Tozzola, A. Tacca et al., "Photo-electrochemical properties of nanostructured WO_3 prepared with different organic dispersing agents," *Solar Energy Materials & Solar Cells*, vol. 94, no. 5, pp. 788–796, 2010.

[16] V. Cristino, S. Caramori, R. Argazzi, L. Meda, G. L. Marra, and C. A. Bignozzi, "Efficient photoelectrochemical water splitting by anodically grown WO_3 electrodes," *Langmuir*, vol. 27, no. 11, pp. 7276–7284, 2011.

[17] S. Berger, H. Tsuchiya, A. Ghicov, and P. Schmuki, "High photocurrent conversion efficiency in self-organized porous WO_3," *Applied Physics Letters*, vol. 88, no. 20, Article ID 203119, 2006.

[18] A. P. Dowling, "Development of nanotechnologies," *Materials Today*, vol. 7, no. 12, pp. 30–35, 2004.

[19] A. Watcharenwong, W. Chanmanee, N. R. de Tacconi, C. R. Chenthamarakshan, P. Kajitvichyanukul, and K. Rajeshwar, "Anodic growth of nanoporous WO_3 films: morphology, photoelectrochemical response and photocatalytic activity for methylene blue and hexavalent chrome conversion," *Journal of Electroanalytical Chemistry*, vol. 612, no. 1, pp. 112–120, 2008.

[20] S. Jana and R. M. Rioux, "Seeded growth induced amorphous to crystalline transformation of niobium oxide nanostructures," *Nanoscale*, vol. 4, no. 5, pp. 1782–1788, 2012.

[21] J. M. Macak, H. Tsuchiya, A. Ghicov et al., "TiO_2 nanotubes: self-organized electrochemical formation, properties and applications," *Current Opinion in Solid State and Materials Science*, vol. 11, no. 1-2, pp. 3–18, 2007.

[22] M. Paulose, K. Shankar, S. Yoriya et al., "Anodic growth of highly ordered TiO_2 nanotube arrays to 134 μm in length," *The Journal of Physical Chemistry B*, vol. 110, no. 33, pp. 16179–16184, 2006.

[23] N. K. Allam and C. A. Grimes, "Effect of cathode material on the morphology and photoelectrochemical properties of vertically oriented TiO_2 nanotube arrays," *Solar Energy Materials and Solar Cells*, vol. 92, no. 11, pp. 1468–1475, 2008.

[24] L. V. Taveira, J. M. Macák, H. Tsuchiya, L. F. P. Dick, and P. Schmuki, "Initiation and growth of self-organized TiO_2 nanotubes anodically formed in $NH_4F/(NH_4)_2SO_4$ electrolytes," *Journal of the Electrochemical Society*, vol. 152, no. 10, pp. B405–B410, 2005.

[25] J. Shi, J. Chen, Z. Feng et al., "Photoluminescence characteristics of TiO_2 and their relationship to the photoassisted reaction of water/methanol mixture," *The Journal of Physical Chemistry C*, vol. 111, no. 2, pp. 693–699, 2007.

[26] H. D. Zheng, J. Z. Ou, M. S. Strano, R. B. Kaner, A. Mitchell, and K. Kalantar-Zadeh, "Nanostructured tungsten oxide—properties, synthesis, and applications," *Advanced Functional Materials*, vol. 21, no. 12, pp. 2175–2196, 2011.

[27] L. Liang, J. J. Zhang, Y. Y. Zhou et al., "High-performance flexible electrochromic device based on facile semiconductor-to-metal transition realized by $WO_3 \cdot 2H_2O$ ultrathin nanosheets," *Scientific Reports*, vol. 3, article 1936, 2013.

[28] S. Songara, V. Gupta, M. Kumar Patra et al., "Tuning of crystal phase structure in hydrated WO_3 nanoparticles under wet chemical conditions and studies on their photochromic properties," *Journal of Physics and Chemistry of Solids*, vol. 73, no. 7, pp. 851–857, 2012.

[29] F. S. Manciu, J. L. Enriquez, W. G. Durrer, Y. Yun, C. V. Ramana, and S. K. Gullapalli, "Spectroscopic analysis of tungsten oxide thin films," *Journal of Materials Research*, vol. 25, no. 12, pp. 2401–2406, 2010.

[30] E. I. Ross-Medgaarden and I. E. Wachs, "Structural determination of bulk and surface tungsten oxides with UV-vis diffuse reflectance spectroscopy and raman spectroscopy," *The Journal of Physical Chemistry C*, vol. 111, no. 41, pp. 15089–15099, 2007.